Bias dependence of the conductance of Au nanocontacts

Katsuhiro Itakura,* Kenji Yuki, Shu Kurokawa, Hiroshi Yasuda,† and Akira Sakai‡
Mesoscopic Materials Research Center, Kyoto University, Sakyo-ku, Kyoto 606-8501, Japan
(Received 30 April 1998; revised manuscript received 30 April 1999)

The bias dependence of the quantized conductance in Au relay contacts has been studied by measuring the transient conductance in the contact break. Au nanocontacts are known to exhibit sharp peaks in their conductance histograms at and near the quantized positions nG_0 ($G_0=2e^2/h$ and $n=1,2,3,\ldots$). With increasing the bias, we find that the $1G_0$ peak height decreases almost linearly, while the peak position shows no shift and stays at $0.96\pm0.02G_0$. The $2G_0$ peak height also decreases with the bias, and its bias dependence agrees with that of the $1G_0$ peak when the bias is normalized by the disappearance voltage of each peak. We have also measured the distribution of the $1G_0$ plateau length (duration) at various biases and find that the distribution becomes reduced at high biases. However, a small number of plateaus survive even at 2 V, and the average plateau length remains almost bias independent for biases greater than 1.2 V. This result indicates that the suppression of the $1G_0$ peak height at high biases is due to the decrease, not in the plateau lifetime, but in the plateau formation probability. The bias dependence of the $1G_0$ plateau formation is discussed with its relation to the nonlinear conductance in Au nanocontacts. [S0163-1829(99)02439-X]

I. INTRODUCTION

Electron transport through metal nanocontacts has been a subject of intensive experimental and theoretical investigations. These studies have revealed that the conductance of some metal nanocontacts changes discretely in integer multiples of the conductance quantum $G_0=2e^2/h$. This quantized conductance was first observed in scanning tunneling microscopy (STM) contacts of Au,[1–3] and also in mechanically controllable break (MCB) junctions of Cu, Al, and Na.[4,5] Subsequently, a number of experimental studies have been made on the conductance of various metal nanocontacts using STM,[6–19] MCB,[20–25] nanofabricated junctions,[26–28] momentary touching of macroscopic electrodes,[29–32] and relay contacts.[33–35] In these experiments, a nanocontact is formed as a connective neck between macroscopic electrodes. When the electrodes in contact are pulled apart, the contact stretches out and forms a nanowire bridge. At the last stage of contact break, the narrowest constriction becomes the size of atoms and shows the quantized conductance plateaus when there is no electron backscattering.

Although quantized conductance plateaus and steps can be observed in transient conductance traces of breaking metal nanocontacts, the conductance quantization in these contacts is ''statistical'' in a sense that conductance plateaus and steps appear only statistically, and their shapes and positions vary in each contact break. The statistical nature of conductance plateaus has been first pointed out by Krans *et al.*[5] and attributed to a variety of deformation process for metal nanocontacts. When the size of a contact becomes comparable with that of atoms, the contact deformation proceeds discretely by repeating elastic elongation and subsequent abrupt rearrangement of contact atoms. The presence of such an abrupt atomic rearrangement during the contact break has been experimentally verified by Rubio, Agraït, and Vieira.[12] The conductance shows a step at each atomic rearrangement while it takes a plateau when the nanocontact undergoes elastic elongation in a relaxed state. Since there should be many such relaxed states of different contact geometry, the actual deformation path through them cannot be uniquely determined and should change in each contact break. This explains why conductance plateaus and their positions are not reproducible. Nevertheless, the deformation path may not be completely random but likely to pass through some preferred geometries which have higher stability than others. Then, conductance plateaus corresponding to these geometries appear most frequently and would accumulate to form peaks when a large number of conductance data are used to construct a conductance histogram. Such conductance peaks have been observed in conductance histograms of some metal nanocontacts.[29,31,16,23,34,35] In particular, the histogram of Au shows a large peak at $1G_0$ and also smaller peaks at $2G_0,3G_0,\ldots$. A large $1G_0$ peak indicates a remarkable stability of the $1G_0$ states of Au. In fact, the fracture strength of these states is comparable to the ideal strength of a bulk Au crystal.[12]

In our previous experiment,[34] we have shown that the $1G_0$ peak of Au exhibits strong bias dependence, and its peak height decreases under high bias. The peak disappears at 1.9 V under a contact current of 137 μA. This result implies that the $1G_0$ state of Au becomes less stable at higher biases. However, the mechanism(s) of this peak suppression has not been well understood. In addition, the observed $1G_0$ conductance at high biases apparently contradict to the nonlinear conductance in Au nanocontacts reported by Costa-Krämer *et al.*[31,36] According to their STM experiments on Au nanocontacts, the differential conductance of nG_0 states does not remain constant but increases with the bias. For example, the conductance of the $1G_0$ state nearly exceeds $2G_0$ at 0.25 V. The nonlinear conductance starts at around 0.1 V, and the experimental I-V characteristics can be fitted to $I=a_1V+a_2V^2+a_3V^3$, where the V^3 term dominates the contact current at high biases. The linear $1G_0$ conductance or the $1G_0$ conductance peak at biases well above 0.1 V are thus quite unexpected from the nonlinear I-V characteristics.

Conductance of metal nanocontacts has been calculated

 ©1999 The American Physical Society

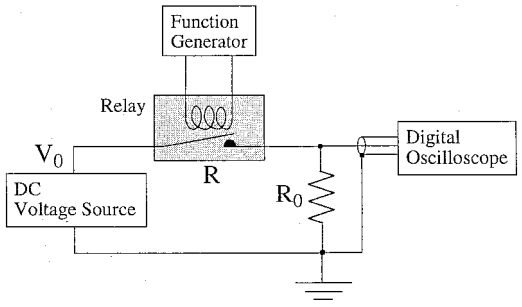

FIG. 1. Schematic diagram of the conductance measuring system. A transient conductance of a relay is measured with a fast digital oscilloscope which monitors the voltage drop across a current-sensing resistor R_0 connected in series with the relay.

for various contact models[37–48] and for simulated contact geometries.[49–57] Unfortunately, most of these studies are concerned with the conductance at low biases, and no theoretical analyses have been made on metal nanowires under high bias. One exception is the work by Pascual, Torres, and Sáenz[40] who calculated the nonlinear conductance for a cylindrical ballistic contact up to a bias comparable to the Fermi energy. However, it is not clear whether actual Au nanocontacts formed in breaking contacts can be well approximated by a simple cylindrical contact since the $2G_0$ peak, which must be absent for axially symmetric contacts, is actually observed in Au nanocontacts.

In this paper we present our experimental results on the bias dependence of the conductance of Au nanocontacts. A change in the $1G_0$ peak height with bias has been investigated in more detail than in our previous experiment.[34] The distribution of the $1G_0$ plateau length (duration) has also been measured as a function of bias. This measurement of the plateau length is quite important since it enables us to separate out the influence of the plateau length on the bias dependence of the $1G_0$ peak height.

II. EXPERIMENT

As in our previous experiments,[33,34] we employed relay contacts for producing metal nanocontacts. All measurements were carried out in air at room temperature. Figure 1 shows a schematic of our experimental setup. A fixed current-sensing resistor (resistance R_0) is connected in series with a relay and a constant dc voltage V_0 is applied to the circuit from a voltage source. A voltage drop V_m across the resistor is monitored by a fast digital oscilloscope with a sampling rate of one data point per 2 ns, and the measured V_m is converted to a relay conductance G through an equation, $G=(1/R_0)[V_m/(V_0-V_m)]$. Similar setup has also been employed by Landman *et al.*[30] and Hansen *et al.*[35] in their conductance measurements. We used nominal 1000Ω ($R_0=998\Omega$, after taking into account the input impedance of the oscilloscope) and 200Ω resistors for R_0. A higher R_0 gives good S/N ratio but slows down the transient response of the measuring system. For 1000Ω and 200Ω resistors, the time constant of our measuring system is estimated to be 32 and 6 ns, respectively. Since short plateaus cannot be accurately monitored with large time constant, a 200Ω resistor was used in all measurements of the plateau length described in Sec. III B.

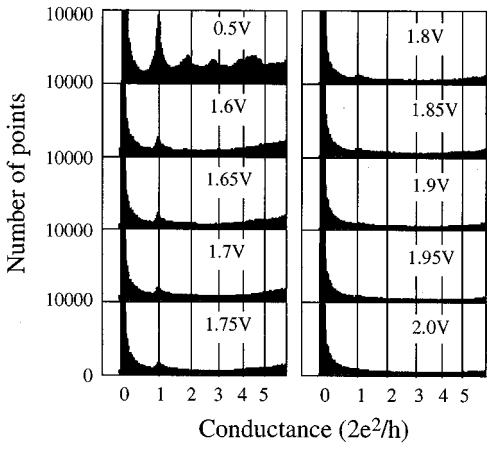

FIG. 2. Conductance histograms at high biases. A histogram obtained at $V_0=0.5$ V and nine histograms from $V_0=1.6$ to 2.0 V are shown in this figure. Note that the bias voltage V_b for the $1G_0$ peak is approximately 7% lower than V_0 indicated in each histogram.

When the relay electrodes are put into contact, the moving electrode bounces off several times and makes a ''chattering'' noise. To avoid this chattering, our conductance measurements were made only during the contact break. Also we employed no switching circuits for activating a relay coil. Instead, a sawtooth signal from a function generator was used to open and close the relay contact. A negative slope of the sawtooth signal was kept as small as possible to minimize inductive noises from the coil.

Since the relay is in series with the resistor R_0, the bias voltage V_b of the contact is always smaller than V_0 by the voltage drop V_m across R_0. Therefore, $V_b=V_0-V_m=V_0/(1+GR_0)$. This means that the bias voltage V_b depends on the conductance G and thus changes with G during the contact break. The voltage drop amounts to 7% of V_0 for a 1000Ω resistor and at $G=1G_0$. This distinction between V_b and V_0 has to be taken into account when we discuss the bias dependence of the conductance in Sec. III A. However, no such distinction is necessary for a 200Ω resistor since the difference between V_b and V_0 is less than 2% at $G=1G_0$.

The relays used in this experiment are commercial Au-contact relays which have Ag electrodes covered with a Au clad layer. The thickness of this layer is typically ~8 μm. The compositional analysis by electron-probe-microanalysis (EPMA) shows that the Au clad layer contains 9 wt% Ag (and a small amount of Si [0.09 wt%)]. The influence of Ag impurities on the conductance will be discussed in the next section.

III. EXPERIMENTAL RESULTS

A. Bias dependence of the conductance histogram

Figure 2 shows a series of histograms obtained on a Au relay at room temperature by increasing V_0 from 1.6 to 2.0 V by a 50-mV step. A histogram at $V_0=0.5$ V is also shown for comparison. Note that the bias voltage V_b for the $1G_0$ peak is slightly different from V_0 and approximately $0.93V_0$, as

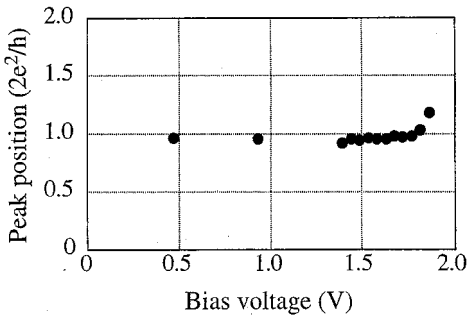

FIG. 3. Peak position of the $1G_0$ conductance peak of Au plotted against the bias voltage.

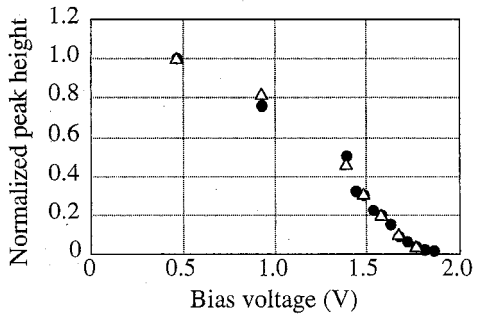

FIG. 4. Observed $1G_0$ peak height plotted against the bias voltage. The peak height is normalized at its value at $V_0=0.5\,\mathrm{V}$ ($V_b=0.465\,\mathrm{V}$). Closed circles and open triangles represent two data sets obtained on different relays.

noted in Sec. II. Each histogram is constructed from 2000 conductance traces and subjected to the differential nonlinearity correction described by Hansen *et al.*[35] We counted in all conductance traces including featureless traces which show no plateaus and steps. These featureless traces contribute to an over-scaled zero conductance peak in each histogram.

When repeating many ON-OFFs under a high-voltage/high-current condition, some degradations of the contact electrodes may take place with time, which would give a false bias dependence if we simply increase the bias with time and measure the conductance. In order to eliminate this artifact, we first recorded only 200 traces at each V_0 and then repeated this series of measurements 10 times to accumulate 2000 traces. Then the degradation effects, even when they exist, would give the same influence in all histograms, and the relative change in the conductance peak height properly represents the true bias dependence.

As described in Sec. II, the Au clad layer in our relay contacts contains 9 wt % Ag. These Ag atoms, however, seem to have no significant influence at least on our nG_0 peaks since the observed conductance histogram at 0.5 V is in good agreement with the reported histogram of Au.[29,35] From this result, we believe that the nanocontacts contributing to the observed nG_0 peaks are free from Ag atoms and consist of Au atoms. The absence of impurity effects in the conductance histogram has also been reported on Au contacts containing 5 % Co.[35] According to the theoretical study of the effects of localized scatterers in nanowires,[52] the $1G_0$ step, and hence the $1G_0$ peak, becomes significantly smeared out when there are localized scatterers (impurities) in the constriction. A sharp $1G_0$ peak in the top panel of Fig. 2 shows that this is not the case for our Au relay contacts.

The bias dependence of the histogram shown in Fig. 2 well reproduces the results previously obtained in Ref. 34. The $1G_0$ peak height decreases with increasing the bias, while the peak position remains unshifted. To make these result more quantitative, we made a Gaussian fit to the peak and numerically obtained the peak position and the peak height. When performing peak fitting, we subtracted a background assuming a form A/V_m+B, where A and B are constants. The first term represents the tail of the zero conductance peak. The position and the height of the $1G_0$ peak obtained from the peak fitting are plotted in Figs. 3 and 4, respectively, as a function of the bias voltage V_b. The solid circles in Figs. 3 and 4 are obtained on the same relay. The open triangles in Fig. 4 obtained on a different relay are in excellent agreement with solid circles, showing essentially no difference between conductance data on different relays. Peak positions corresponding to open triangles in Fig. 4 are not plotted in Fig. 3 since they entirely overlap with solid circles.

Figure 3 clearly demonstrates that the peak position shows no bias dependence and stays constant up to 1.8 V. There can be seen a slight shift to higher conductance at $V_b \geqslant 1.8\,\mathrm{V}$. However, the peak fitting in this high-bias regime has lower reliability because the conductance peak becomes quite small and almost buried in the background. It is thus difficult at this time to conclude a peak shift at $V_b \geqslant 1.8\,\mathrm{V}$. For biases below 1.8 V, the conductance peak stays at $0.96\pm0.02G_0$. This peak position is in good agreement with the reported position of the $1G_0$ peak of Au in previous experiments.[7,9,31,35] A small deviation of the peak position from the exact quantized value has been discussed by some authors and attributed to the residual resistance[7,35] arising from internal disorder in the nanowire,[43] or the additional electron reflection due to an abrupt contact geometry.[38] From our experimental results, we cannot conclude which one of these mechanisms is responsible for the observed 4% peak shift from $1G_0$. Whatever the source of this deviation is, it must be insensitive to the bias voltage since the observed peak position shows no changes with bias.

We note that the height of each conductance peak changes with the number of traces used to construct the histogram. The peak grows up when more data are added to the histogram, and the growth rate may not necessarily be the same for different relays. A normalization of peak height is thus necessary for obtaining physically meaningful bias dependence. For each data set, we used the peak height at $V_0=0.5\,\mathrm{V}$ as a reference and normalized other peak heights by it. Figure 4 shows the resulting bias dependence of the normalized peak height. When the bias voltage increases, the peak height decreases almost linearly up to $V_b\sim1.8\,\mathrm{V}$. Above 1.8 V, however, the decrease in peak height appears to slow down. This makes it quite difficult to accurately determine the critical bias voltage V_{bc} at which the $1G_0$ peak disappears. At least, V_{bc} is close to 2 V.

An interesting result can be obtained when we compare the bias dependence of the $1G_0$ peak height with that of the $2G_0$ peak. It is relatively difficult to measure the bias dependence of the $2G_0$ peak because of its small peak height even at low biases. Nevertheless, some data were obtained on a

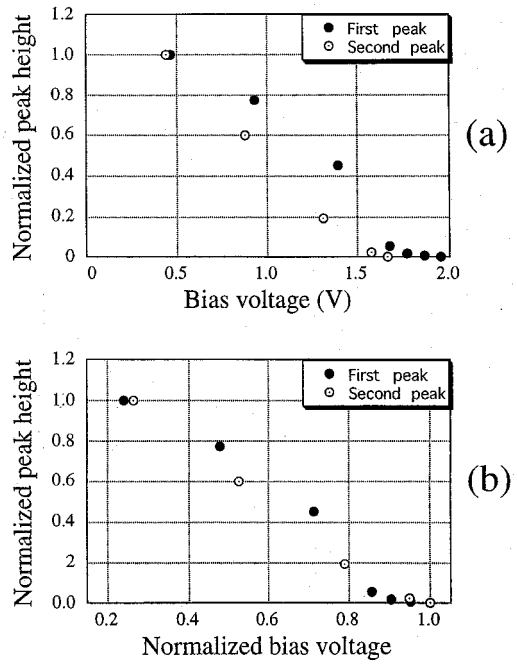

FIG. 5. Bias dependence of the normalized peak height for the first $1G_0$ peak (closed circles) and for the second $2G_0$ peak (open circles) (a), and the same data plotted against the normalized bias voltage (b). The normalized bias voltage in (b) is defined as V_b/V_{bc} where V_{bc} represents the bias at which the conductance peak disappears.

Au-contact relay of quite low background. Figure 5(a) compares the observed bias dependence of the normalized $1G_0$ peak height with that of the $2G_0$ peak. In Fig. 5(a), the behavior of the $1G_0$ peak height is in good agreement with the result shown in Fig. 4. The $2G_0$ peak also displays a quite similar bias dependence: the peak height first decreases almost linearly with bias, tends to slow down at $V_b > 1.5$ V, and finally vanishes at around $V_b = 1.7$ V. The similarity between two plots in Fig. 5(a) can be more clearly visualized when we replot the peak height against a reduced bias V_b/V_{bc} where V_{bc} denotes the critical bias voltage for the peak disappearance. Values of V_{bc} cannot be accurately determined because of the weak bias dependence of the $1G_0$ and $2G_0$ peak heights near their V_{bc}. Nevertheless, we can obtain 2.0 and 1.7 V as a crude estimation of V_{bc} for $1G_0$ and $2G_0$ peaks, respectively. Figure 5(b) shows the universal plot of the peak height. It can be seen in the figure that all data points lie on a single curve, i.e., the conductance peak height shows universal bias dependence. A small deviation from the universal curve may be due to an uncertainty in V_{bc}. Such a universal behavior naturally suggests that the bias dependence of the nG_0 peak height is governed by the same mechanism. The peak suppression at high biases takes place equally for all peaks, irrespective of their quantized positions.

B. Plateau length and its bias dependence

There are two factors that contribute to form the $1G_0$ peak. One is the formation probability of $1G_0$ plateaus, and another is their duration (plateau length). The peak grows up when the plateau appears more frequently and extends longer. Consequently, the $1G_0$ peak height can be written as $Ap\langle\tau\rangle$, where $\langle\tau\rangle$ and p are the average plateau length and the formation probability of $1G_0$ plateaus, respectively, and A is an appropriate proportionality constant. The observed suppression in the peak height, therefore, means either $\langle\tau\rangle$ or p, or both, decreases with increasing the bias.

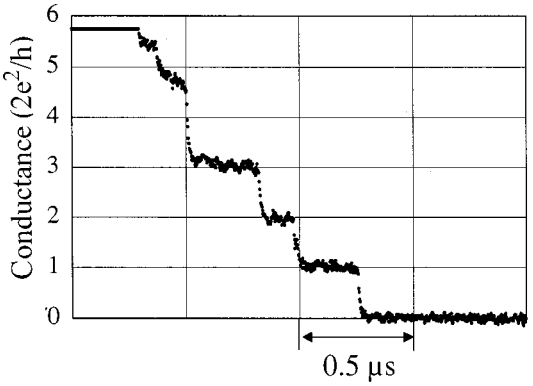

FIG. 6. Typical conductance trace recorded at $V_0 = 1$ V with a 200Ω resistor as R_0 in Fig. 1. Each conductance step shows no appreciable exponential tail at its lower edge.

To separate out the bias dependence of $\langle\tau\rangle$, we measured the length (duration) of $1G_0$ plateaus at various bias voltages. As mentioned in Sec. II, we used a 200Ω resistor as R_0 in Fig. 1 to reduce the time constant of conductance measurement down to 6 ns. A typical conductance trace is shown in Fig. 6. Compared with traces (obtained with a 1000Ω resistor) in our previous work, the trace in Fig. 6 displays sharp conductance steps with no appreciable exponential tail at their lower edges. However, the S/N ratio becomes worse for $R_0 = 200\Omega$, and data points in plateaus appear to show some fluctuations. The $1G_0$ plateau length was measured by counting the number of data points which lie within a conductance window $0.8G_0 - 1.2G_0$ in each conductance trace. A rather wide window was used to cover all data points in noisy plateaus.

Figure 7 shows experimental histograms of the $1G_0$ plateau length for bias voltages from 0.5 to 2.0 V. To obtain

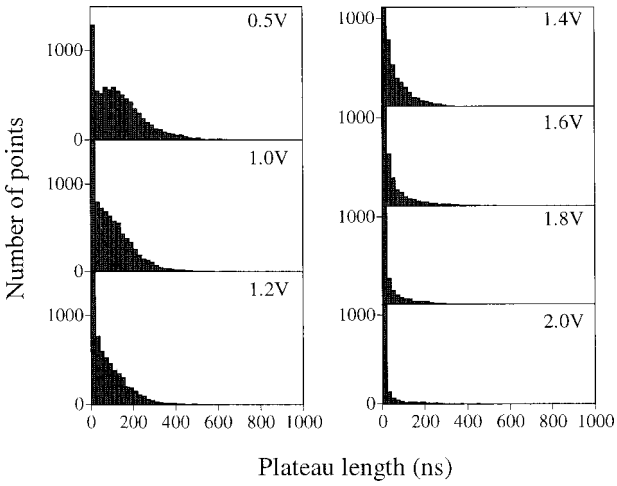

FIG. 7. Distributions of the $1G_0$ plateau length obtained at different biases. A single-tall column in the first bin is due to featureless traces with no plateaus.

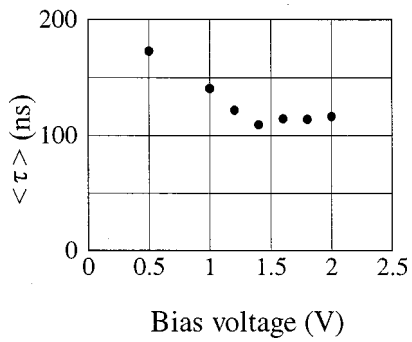

FIG. 8. Bias dependence of the average $1G_0$ plateau length $\langle\tau\rangle$. It shows little bias dependence for $V_b > 1.2$ V.

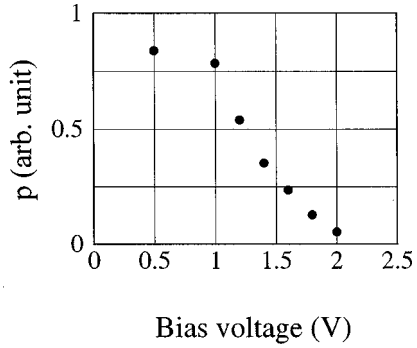

FIG. 9. Bias dependence of the $1G_0$ plateau formation probability p. The $1G_0$ peak height is proportional to the product $p\langle\tau\rangle$. Since $\langle\tau\rangle$ is almost constant at high biases, the decrease in p accounts for the observed $1G_0$ peak-height suppression.

good statistics, 10 000 traces for each V_0, taken from four data sets, were used to construct these histograms. The bin width is 20 ns, approximately three times longer than the time constant of the conductance measurement. A single peak in the first bin in each histogram is mostly due to featureless traces. Even though these traces exhibit no plateaus, they still have a few data points within the conductance window and produce a tall column in the first bin. At 0.5 V, the plateau-length distribution shows a broad maximum at around 100 ns and a long tail extending to $\sim$ 600 ns. The shape of this distribution resembles the Wigner distribution reported by Costa-Krämer *et al.*[31] for the distribution of the $1G_0$ plateau elongation. However, quantitative comparison between their distribution and ours in Fig. 7 cannot be made at this time because we cannot know the speed of contact break in our relay contacts. Rough estimation of the speed of electrode separation, based on the transient ON/OFF time of these relays, implies that it is at least orders of magnitude faster than the speed of tip retraction used in STM (Refs. 31 and 19) and MCB (Ref. 25) experiments.

As the bias is increased to 1 V, the distribution no longer shows a maximum and becomes a decreasing function of the plateau length. The number of featureless plateaus and of short plateaus less than 100 ns grow up while the appearance of longer plateaus is relatively suppressed. As the bias is further increased, the distribution approaches to a smoothly decaying behavior and becomes an exponential-like distribution at 1.4 V. In contrast, the column height in the first bin increases rapidly with bias (it already overscales at 1.2 V). It is just as if the distribution ''collapses'' to the first-bin peak with increasing the bias. For $V_b > 1.5$ V, the distribution is totally reduced, leaving only a large peak in the first bin. However, the tail part of the distribution does not die out completely, and the distribution has small but nonzero values for plateaus greater than 200 ns even at 2 V. This result indicates that not all of $1G_0$ plateaus become short-lived at high biases. A small number of $1G_0$ plateaus still show the plateau length comparable to that at lower biases.

We show in Fig. 8 the average plateau length $\langle\tau\rangle$ as a function of bias voltage. We simply calculated $\langle\tau\rangle$ as an arithmetic average of distribution, i.e., $\langle\tau\rangle = \Sigma_{i=2} n_i\tau_i / \Sigma_{i=2} n_i$, where n_i and τ_i are the column height and the plateau length in the ith bin, respectively. The data in the first bin ($i=1$) were not included in the calculation. As seen in the figure, $\langle\tau\rangle$ first decreases linearly as the bias increases but becomes almost bias independent for $V_b > 1.2$ V. This behavior of $\langle\tau\rangle$ at high biases is clearly due to the tail of the distribution which survives up to 2 V. As mentioned in the beginning of this section, the $1G_0$ peak height is proportional to $p\langle\tau\rangle$. A comparison of Figs. 8 and 4 clearly indicates that $\langle\tau\rangle$ shows different bias dependence from that of the $1G_0$ peak height. Therefore, $\langle\tau\rangle$ is not responsible for the observed $1G_0$ peak suppression at high biases.

C. Formation probability of $1G_0$ plateaus

We next consider the formation probability p of $1G_0$ plateaus, which is another factor contributing to the $1G_0$ peak height. In each histogram in Fig. 7, the sum of all columns except the first one represents the total number of observed $1G_0$ plateaus (of different length). Its ratio to the total number of traces thus gives the formation probability of the $1G_0$ plateau, i.e., $p = \Sigma_{i=2} n_i / \Sigma_{i=1} n_i$. The probability p obtained in this way is displayed in Fig. 9. It shows a slight reduction when the bias is increased from 0.5 to 1 V and then decreases rapidly. This decrease in p corresponds to the collapse of the distribution to the first-bin peak which quickly increases its height. As mentioned in the beginning of Sec. III B, the product $p\langle\tau\rangle$ must be proportional to the $1G_0$ peak height. We calculated from Figs. 8 and 9 this product and confirmed that its bias dependence indeed well agrees with that of the $1G_0$ peak height shown in Fig. 4. Since $\langle\tau\rangle$ changes little for $V_b > 1.2$ V, the bias dependence of the $1G_0$ peak height in this bias range is dominated by that of p. The result in Fig. 9 clearly shows that the $1G_0$ peak suppression is essentially due to the decrease in p at high biases.

IV. DISCUSSION

There are two issues to be discussed concerning our experimental results on the high-bias conductance of Au nanocontacts. The first one is the problem of nonlinear conductance mentioned in Sec. I, and the second is the suppression in the $1G_0$ peak height, or in the plateau formation probability p.

We first consider the nonlinear conductance. STM experiments[31,37] on Au nanocontacts have revealed that the I-V curves measured at $1G_0$ plateaus become nonlinear at around 0.1 V, and the contact current increases with V as

$\sim V^3$. If all $1G_0$ states show such nonlinear conductance, the $1G_0$ peak in a histogram would continuously shift to higher conductance with bias, and plateaus would appear at $G > 1G_0$ in conductance traces. However, our conductance histograms in Fig. 2 show no such peak shift, nor emergence of new peaks at $G > 1G_0$. Also, conductance traces give no clear evidence of plateaus which correspond to the nonlinear conductance. These experimental observations suggest that most nonlinear $1G_0$ states become unstable under high bias and too short lived to make an appreciable contribution to the histogram. Their instability under high bias is not unlikely since the current density in the nonlinear regime grows up quite rapidly with V_b, which can result in contact destruction by electromigration or local Joule heating. In their experiments on thin-film Ti and Nb nanocontacts at room temperature, Schmidt *et al.*[28] find that both electromigration and Joule heating contribute to contact instability under high current density. In our Au nanocontacts, it is rather difficult to estimate the magnitude of these effects since no quantitative information is available on a ''base'' region of a nanowire neck where ballistic electrons are scattered by contact atoms and dissipate their kinetic energy. If we assume the size of this region to be comparable to the electron mean free path $\sim$ 6 nm estimated from the resistivity data, then the current density in the base region reaches $j \sim 5 \times 10^8$ A/cm^2 at 0.5 V for nonlinear $1G_0$ states with nonlinear coefficients reported in Ref. 31. Since instantaneous contact destruction is observed on Ti nanocontacts at $j > 10^8$ A/cm^2,[28] nonlinear $1G_0$ states are likely to become unstable against electromigration under high bias.

On the other hand, the temperature rise in the base region, estimated by assuming the Wiedemann-Franz law, remains $\Delta T \sim 200$ K for nonlinear $1G_0$ states at 0.5 V but quickly increases to $\Delta T \sim 900$ K at 1 V. Therefore, the Joule heating may also be important for $V_b > 1$ V. However, our experiments on Au nanocontacts at 77 K (Ref. 34) and at 4 K (Ref. 58) show little evidence for improved stability of nonlinear states. Although the possibility of local overheating in nanocontacts cannot be completely ruled out, these results at lower temperatures suggest that the Joule heating may not be a major source of instability of Au nanocontacts under high bias.

Taking into account bias-induced instabilities along with the nonlinear conductance, we have to consider for each $1G_0$ state two threshold bias voltages V_n and V_i for the onset of nonlinear conduction and of contact instability, respectively. Instability of nonlinear $1G_0$ states suggests that V_i is higher than but not much different from V_n. For most $1G_0$ states, $V_n \sim 0.1$ V as found by STM experiments,[36] and perhaps V_i is at most $\sim$ 0.5 V due to electromigration and Joule heating as discussed above. However, not all $1G_0$ states have $V_i \leqslant 0.5$ V since otherwise, they would become all unstable at 1 V, and hence no $1G_0$ peaks would be observed in histograms in Fig. 2. Therefore, the $1G_0$ peaks in Fig. 2 constitute an experimental evidence that there exits some $1G_0$ states which have high onset voltages and maintain linear conductance up to high biases. These stable $1G_0$ states are considered to be responsible for $1G_0$ plateaus and the $1G_0$ peak for $V_b > 1$ V. Then, the probability $p(V_b)$ of the $1G_0$ plateau formation represents the fraction of $1G_0$ states which satisfies the criteria V_n, $V_i > V_b$. In this sense, p represents the ''survival rate'' of the $1G_0$ state against current-induced instabilities. The decrease in p displayed in Fig. 9 shows that fewer $1G_0$ states satisfy the above criteria as V_b increases.

Experiments on nonlinear conductance clearly indicate $V_n < V_i$. However, since I-V measurements can only be performed on stable contacts, these experiments cannot rule out the presence of some $1G_0$ states for which $V_i < V_n$. In fact, estimated current density and temperature rise at $V_b = 2$ V are $j \sim 4 \times 10^8$ A/cm^2 and $\Delta T \sim 400$ K, respectively. It may thus not be unlikely that some $1G_0$ states are unstabilized near 2 V even before their onset of nonlinear conduction. However, we consider $V_n \leqslant V_i$ for most $1G_0$ states, and hence the bias dependence of p reflects the distribution of V_n. It is because this interpretation of $p(V_b)$ accounts for the observed universal bias dependence for the $1G_0$ and $2G_0$ peak heights shown in Fig. 5. According to STM experiments,[36] $1G_0$ and $2G_0$ states display almost the same nonlinear behavior. This result suggests that $1G_0$ and $2G_0$ states have similar distribution of V_n and hence show similar bias dependence of their peak height if $p(V_b)$ represents the distribution of V_n.

It is not yet clear why some $1G_0$ states have so high V_n and V_i that they can show linear conductance up to 2 V, while others become nonlinear and unstable below 0.5 V. Some clues for such stable and ''rigid'' $1G_0$ states, however, can be obtained from recent direct observations of contact atoms by high-resolution transmission electron microscopy.[59–62] Ohnishi, Kondo, and Takayanagi (Ref. 61) has demonstrated that a Au contact at its nG_0 state consists of n chains of Au atoms. In particular, the $1G_0$ contact consists of a single linear array of 2–3 Au atoms. Recent MCB experiment[25] and theoretical simulation[57] prove high stability of such an atomic chain of Au atoms. For example, Yanson *et al.*[25] found that some atomic chains can sustain 80 μA under 1 V. These results make a single-atom chain the most probable contact geometry for rigid $1G_0$ states. However, the final answer cannot be obtained until the linear conductance of a single chain under high bias is confirmed either by direct conductance measurements or by conductance calculations.

V. CONCLUSION

We have studied the bias dependence of the $1G_0$ conductance peak of Au relay contacts and analyzed the distribution of the $1G_0$ plateau length. We find that the $1G_0$ peak height decreases almost linearly with increasing the bias, while the peak position makes no shift and stays at $0.96 \pm 0.02 G_0$. The same behavior is also observed for the $2G_0$ peak height, suggesting a universal bias dependence of the peak height. Under high bias, the majority of conductance traces become featureless and show no conductance plateaus. However, a small number of long plateaus survive even at high biases and lead to the average plateau length $\langle \tau \rangle$ which is almost bias independent for $V_b > 1.2$ V. On the other hand, the formation probability p of the $1G_0$ plateau is found to simply decrease with increasing the bias. Comparison of the bias dependence of the $1G_0$ peak height with those of p and $\langle \tau \rangle$ shows that the suppression of the $1G_0$ peak is due to the decrease in p.

In our conductance traces and histograms, we observed no

features which can be attributed to the nonlinear conductance. This result suggests that most nonlinear $1G_0$ states become unstable under high bias, due to growing current density, and do not contribute to high-bias conductance histograms. The bias dependence of the $1G_0$ peak height, or the probability p, can then be interpreted as representing the survival rate of the $1G_0$ state against the onset of nonlinear conductance. We also find that some $1G_0$ states can maintain linear conductance even at 2 V. A single-atom chain of Au recently observed in electron microscopy is by far the likeliest candidate for the atomic structure of such stable and rigid $1G_0$ states.

*Present address: Sumito Electric Industries, Itami 664, Japan.
†Present address: Texas Instruments Japan, Tokyo 108-0023, Japan.
‡Author to whom correspondence should be addressed. Electronic address: sakai@mesostm.mtl.kyoto-u.ac.jp

[1] N. Agraït, J. G. Rodrigo, and S. Vieira, Phys. Rev. B **47**, 12 345 (1993).
[2] J. I. Pascual, J. Méndez, J. Gómez-Herrero, A. M. Baró, N. García, and Vu Thien Binh, Phys. Rev. Lett. **71**, 1852 (1993).
[3] L. Olesen, E. Læsgarrd, I Stensgaard, F. Besenbacher, J. Schiøtz, P. Stolze, K. W. Jacobsen, and J. K. Nørskov, Phys. Rev. Lett. **72**, 2251 (1994).
[4] J. M. Krans, C. J. Muller, I. K. Yanson, Th. C. M. Govaert, R. Hesper, and J. M. van Ruitenbeek, Phys. Rev. B **48**, 14 721 (1993).
[5] J. M. Krans, J. M. van Ruitenbeek, V. V. Fisun, I. K. Yanson, and L. J. de Jongh, Nature (London) **375**, 767 (1995).
[6] J. I. Pascual, J. Méndez, J. Gómez-Herrero, A. M. Baró, N. García, Uzi Landman, W. D. Luedtke, E. N. Bogachek, and H.-P. Cheng, Science **267**, 1793 (1995).
[7] M. Brandbyge, J. Schiøtz, M. R. Sorensen, P. Stolze, K. W. Jacobsen, J. K. Nørskov, L. Olesen, E. Læsgarrd, I. Stensgaard, and F. Besenbacher, Phys. Rev. B **52**, 8499 (1995).
[8] N. Agraït, G. Rubio, and S. Vieira, Phys. Rev. Lett. **74**, 3995 (1995).
[9] D. P. E. Smith, Science **269**, 371 (1995).
[10] Z. Gai, Y. He, H. Yu, and W. S. Yang, Phys. Rev. B **53**, 1042 (1996).
[11] A. Stalder and U. Dürig, Appl. Phys. Lett. **68**, 637 (1996); Probe Microscopy **1**, 135 (1998).
[12] G. Rubio, N. Agraït, and S. Vieira, Phys. Rev. Lett. **76**, 2302 (1996).
[13] C. Sirvent, J. G. Rodrigo, S. Vieira, L. Jurczyszyn, N. Mingo, and F. Flores, Phys. Rev. B **53**, 16086 (1996).
[14] J. L. Costa-Krämer, Phys. Rev. B **55**, R4875 (1997).
[15] J. L. Costa-Krämer, N. García, and H. Olin, Phys. Rev. B **55**, 19 (1997).
[16] J. L. Costa-Krämer, N. García, and H. Olin, Phys. Rev. Lett. **78**, 4990 (1997).
[17] C. Untiedt, G. Rubio, S. Vieira, and N. Agraït, Phys. Rev. B **56**, 2154 (1997).
[18] C. Z. Li, H. Sha, and N. J. Tao, Phys. Rev. B **58**, 6775 (1998).
[19] W. B. Jian, C. S. Chang, W. Y. Li, and T. T. Tsong, Phys. Rev. B **59**, 3168 (1999).
[20] C. Zhou, C. J. Muller, M. R. Deshpande, J. W. Sleight, and M. A. Reed, Appl. Phys. Lett. **67**, 1160 (1995).
[21] C. J. Muller, J. M. Krans, T. N. Todorov, and M. A. Reed, Phys. Rev. B **53**, 1022 (1996).
[22] E. Scheer, P. Joyez, D. Esteve, C. Urbina, and M. H. Devoret, Phys. Rev. Lett. **78**, 3535 (1997).
[23] A. I. Yanson and J. M. van Ruitenbeek, Phys. Rev. Lett. **79**, 2157 (1997).
[24] E. Scheer, N. Agraït, J. C. Cuevas, A. Levy Yeyati, B. Ludoph, A. Martín-Rodero, G. R. Bollinger, J. M. van Ruitenbeek, and C. Urbina, Nature (London) **394**, 154 (1998).
[25] A. I. Yanson, G. R. Bollinger, H. E. van den Brom, N. Agraït, and J. M. van Ruitenbeek, Nature (London) **395**, 783 (1998).
[26] E. S. Snow, D. Park, and P. M. Campbell, Appl. Phys. Lett. **69**, 269 (1996).
[27] T. Junno, S.-B. Carlsson, H. Xu, L. Montelius, and L. Samuelson, Appl. Phys. Lett. **72**, 548 (1998).
[28] T. Schmidt, R. Martel, R. L. Sandstrom, and Ph. Avouris, Appl. Phys. Lett. **73**, 2173 (1998).
[29] J. L. Costa-Krämer, N. García, P. García-Mochales, and P. A. Serena, Surf. Sci. **342**, L1144 (1995).
[30] U. Landman, W. D. Luedtke, B. E. Salisbury, and R. L. Whetten, Phys. Rev. Lett. **77**, 1362 (1996).
[31] J. L. Costa-Krämer, N. García, P. García-Mochales, P. A. Serena, M. I. Marqués, and A. Correia, Phys. Rev. B **55**, 5416 (1997).
[32] H. Oshima and K. Miyano, Appl. Phys. Lett. **73**, 2203 (1998).
[33] H. Yasuda and A. Sakai, J. Korean Phys. Soc. **31**, S54 (1997).
[34] H. Yasuda and A. Sakai, Phys. Rev. B **56**, 1069 (1997).
[35] K. Hansen, E. Læsgarrd, I. Stensgaard, and F. Besenbacher, Phys. Rev. B **56**, 2208 (1997).
[36] J. L. Costa-Krämer, N. García, M. Jonson, I. V. Krive, H. Olin, P. A. Serena, and R. I. Schehkter, in *Nanoscale Science and Technology*, Vol. 348 of *NATO Advanced Study Institute Series E: Applied Sciences*, edited by N. García, M. Nieto-Vesperinas, and H. Rohrer (Kluwer Academic, Dordrecht, 1998), p. 1.
[37] J. A. Torres and J. J. Sáenz, Phys. Rev. Lett. **77**, 2245 (1996).
[38] J. A. Torres, J. I. Pascual, and J. J. Sáenz, Phys. Rev. B **49**, 16 581 (1994).
[39] A. García-Martín, J. A. Torres, and J. J. Sáenz, Phys. Rev. B **54**, 13 448 (1996).
[40] J. I. Pascual, J. A. Torres, and J. J. Sáenz, Phys. Rev. B **55**, R16 029 (1997).
[41] J. M. van Ruitenbeek, M. H. Devoret, D. Esteve, and C. Urbina, Phys. Rev. B **56**, 12 566 (1997).
[42] N. D. Lang, Phys. Rev. Lett. **79**, 1357 (1997).
[43] P. García-Mochales and P. A. Serena, Phys. Rev. Lett. **79**, 2316 (1997).
[44] D. Sánchez-Portal, C. Untiedt, J. M. Soler, J. J. Sáenz, and N. Agraït, Phys. Rev. Lett. **79**, 4198 (1997).
[45] C. C. Wang, J.-L. Mozos, G. Taraschi, J. Wang, and H. Guo, Appl. Phys. Lett. **71**, 419 (1997).
[46] J. C. Cuevas, A. Levy Yeyati, and A. Martín-Rodero, Phys. Rev. Lett. **80**, 1066 (1998).
[47] E. Bascones, G. Gómez-Santos, and J. J. Sáenz, Phys. Rev. B **57**, 2541 (1998).
[48] N. Kobayashi, M. Brandbyge, and M. Tsukada, Jpn. J. Appl. Phys. **38**, 336 (1999).
[49] T. N. Todorov and A. P. Sutton, Phys. Rev. Lett. **70**, 2138 (1993); Phys. Rev. B **54**, R14 234 (1996).
[50] A. M. Bratkovsky, A. P. Sutton, and T. N. Todorov, Phys. Rev. B **52**, 5036 (1995).
[51] R. N. Barnett and U. Landman, Nature (London) **387**, 788 (1997).

[52] M. Brandbyge, K. W. Jacobsen, and J. K. Nørskov, Phys. Rev. B **55**, 2637 (1997).
[53] A. Levy Yeyati, A. Martín-Rodero, and F. Flores, Phys. Rev. B **56**, 10 369 (1997).
[54] H. Mehrez and S. Ciraci, Phys. Rev. B **56**, 12 632 (1997).
[55] M. Brandbyge, M. R. Sørensen, and K. W. Jacobsen, Phys. Rev. B **56**, 14 956 (1997).
[56] H. Mehrez, S. Ciraci, C. Y. Fong, and Ş. Erkoç, J. Phys.: Condens. Matter **9**, 10 843 (1997).
[57] M. R. Sørensen, M. Brandbyge, and K. W. Jacobsen, Phys. Rev. B **57**, 3283 (1998).
[58] A. Correia and N. García, Phys. Rev. B **55**, 6689 (1997).
[59] K. Yuki, A. Enomoto, and A. Sakai (unpublished).
[60] T. Kizuka, K. Yamada, S. Deguchi, M. Naruse, and N. Tanaka, Phys. Rev. B **55**, R7398 (1997).
[61] Y. Kondo and K. Takayanagi, Phys. Rev. Lett. **79**, 3455 (1997).
[62] H. Ohnishi, Y. Kondo, and K. Takayanagi, Nature (London) **395**, 780 (1998).